PUSHER PROPELLER INFLUENCE ON A LAMINAR WING TRANSITION LOCATION USING INFRARED THERMOGRAPHY

João Paulo Eguea[1], Gabriel Pereira Gouveia da Silva[1] & Fernando Martini Catalano[1]

[1]Department of Aeronautical Engineering, University of Sao Paulo, Brazil

Abstract

Natural laminar flow wings are presented as a technology capable of improving aircraft performance and fuel consumption reduction. However, a study on the interaction between laminar wings and propellers is necessary for understanding the applicability of the natural laminar flow technology on propeller-driven aircraft. In this work, the impact of a pusher propeller on a laminar wing boundary layer transition position was investigated experimentally in a wind tunnel using an infrared thermography technique. The results showed that the pusher propeller increases the laminar boundary layer extension at low angles of attack. At higher angles of attack, the laminar boundary layer extension presented small or no reduction. Also, the propeller impact on the laminar boundary layer extensions is reduced as the transition front distances from the propeller actuation disk. These results indicate that a pusher propeller might be a better option for aircraft design for wing natural laminar flow in comparison to tractor configuration.

Keywords: natural laminar flow, wind tunnel testing, pusher propeller, infrared thermography

1. Introduction

The aviation market's environmental impact has been one of the great concerns of academics and the industry. Regulations, like International Civil Aviation Organization (ICAO) Resolution A40-18 [1], and the commitment of the aeronautical community on developing new sustainable technologies creates a stable contribution of aviation to man-made emission despite the market growth trend. The International Air Transport Association (IATA) report on technologies that can contribute to reducing aviation emissions indicates that drag reductions due to extended laminar flows may impact aircraft fuel consumption [2]. The wing drag can correspond to up to 18% of the aircraft's total drag [3], drawing the industry and academics attention to the development of natural laminar flow (NLF) and Hybrid laminar flow control (HLFC) designs. Furthermore, the development of all-electric and hybrid propulsion opens room for exploring the wing and propeller interaction for extending the wing laminar boundary layer.

There are plenty of results on the tractor propeller impact on wing boundary layer transition, indicating that the propeller wake and tip vortex creates a cyclical laminar-turbulent boundary layer behind the propeller actuation disk [4, 5, 6, 7]. This behavior results in a drag value between the wing without the propeller influence and a fully turbulent boundary layer. However, the tractor propeller slipstream increases the wing lift curve slope ($\frac{dC_L}{d\alpha}$) maximum lift coefficient ($C_{L_{max}}$) and reduces pressure drag by delaying flow separation due to the increase in the dynamic pressure caused by the propeller [8, 9, 10, 11, 12]. Those effects are higher the lower the propeller advance ratio (J) and the higher the thrust.

The pusher propeller, on the other hand, presents a beneficial effect on wing boundary layer transition. The work from Catalano and Stollery [13, 14] indicated that the pusher propeller delayed laminar boundary layer transition, increasing the laminar separation bubble length inside the slipstream. Further work by Catalano and Maunsell [15] and Catalano [16] also indicated that the pusher propeller

presents the same beneficial effects as the tractor propeller on the lift curve slope, maximum lift coefficient, and pressure drag. The experimental results indicated that the pusher propeller increase the wing aerodynamic efficiency ($\frac{L}{D}$) and delayed turbulent boundary layer separation. Such results are an indication that a synergistic influence between wings and propellers may be achieved for improving aircraft performance.
This work proposes investigating the interaction between a wing designed for natural laminar flow (NLF) with a pusher propeller. Based on the previous results on the beneficial effect of a pusher propeller and the development of all-electric and hybrid distributed propulsion, it is expected to achieve a performance improvement due to the extended laminar boundary layer. In this sense, it is proposed a wind tunnel experiments campaign to measure the influence of the pusher propeller on wing boundary layer transition point using infrared thermography (IRT) technique.

2. Methods

The wind tunnel experiment will be carried out in the LAE-1 tunnel, installed at the Laboratory of Experimental Aerodynamics (LAE) of the Department of Aeronautical Engineering of the University of Sao Paulo [17]. This tunnel has a closed circuit and test section, which allows flow speeds of up to 50 m/s with a turbulence level of 0.21% in its rectangular test section of 1.67 m (width) × 1.29 m (height) × 3 m (length), making it suitable for laminar flow measurements.
The chosen airfoil was designed for laminar flow based on the following requirements:

- $\frac{t}{c}_{max} > 12\%$
- $\frac{x_{tr}}{c}_{min} > 15\%$ at $\alpha \leq 5^{\circ}$
- $5 < \frac{L}{D} < 20$
- No laminar separation
- Symmetric airfoil

The resulting airfoil (Figure 1) presents a $\frac{t}{c}_{max} = 0.156$ and its MSES results showed $\frac{x_{tr}}{c}_{min} = 0.287$.

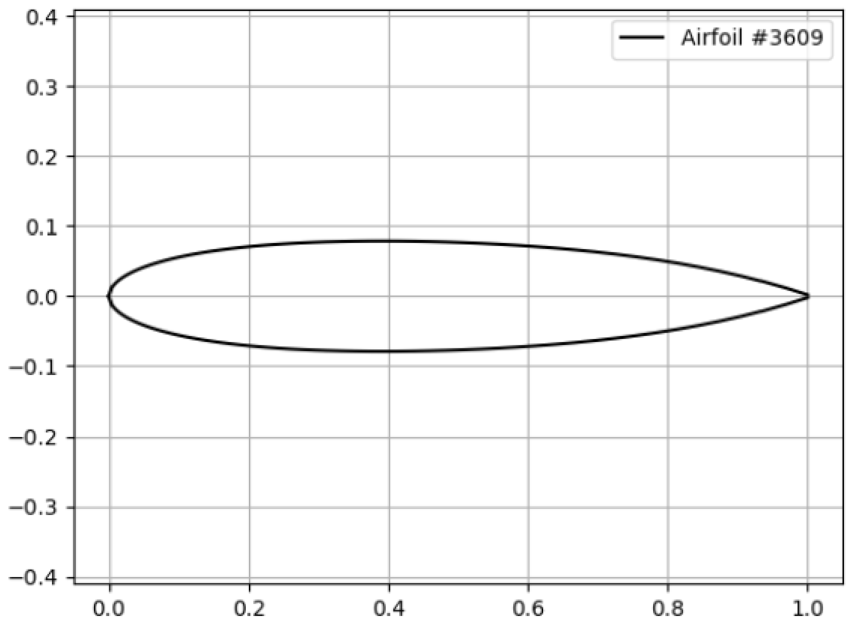

Figure 1 – Selected general laminar airfoil

The IRT technic is a non-intrusive method for detecting boundary layer transition by detecting temperature differences on the heated wing surface using infrared images. The increased heat transfer rate on a turbulent boundary layer due to the flow mixing between the layers reduces the wing surface temperature to less than the laminar flow region, enabling the detection of the transition region. The FLIR A300 infrared camera was used in the experiments (Table 1). The camera software FLIR ThermaCAM Researcher 2.10 is used for post-processing the images and increasing the transition visibility.

Table 1 – Infrared camera specification [18]

Field of View (FOV)	$25^{\circ}x18.8^{\circ}$
Image Frequency	30 Hz
Image Resolution	320 x 240 px
Thermal Sensitivity	$0.05^{\circ}C$
Zoom	1-8 Digital
Communication Rate	3 Hz
Communication Port	IP-Ethernet
Camera age	2010
Output Available	MPEG

Aluminum models are not recommended for IRT experiments. Its high thermal conductivity and infrared reflection on metal surfaces lead to obscured images [19]. The aluminum laminar wing model was covered with a smooth transparent plastic coating to avoid infrared waves' reflection on the model surface. Two sets of three spotlights were installed inside the test chamber for heating the wing surface (Figure 2). Also, two corner fillets were added on the test chamber opposite side for ensuring flow symmetry during the experiments. The proposed setup is shown in Figure 3.

Figure 2 – Installed heating system

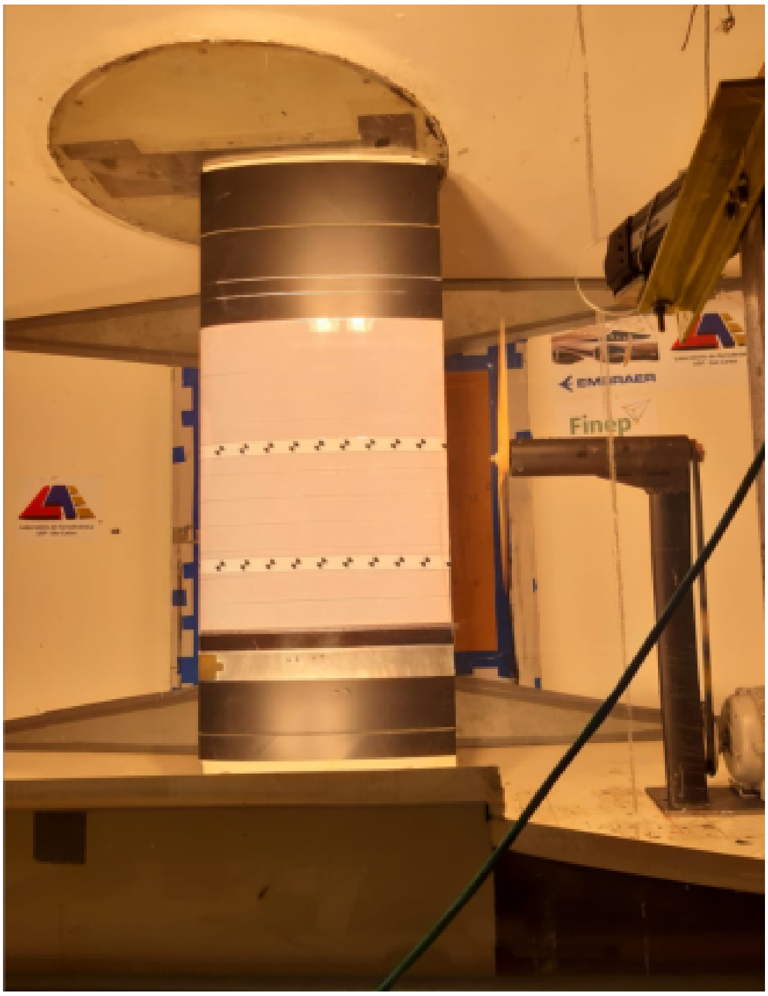

Figure 3 – Wing and propeller installation

The main objective of this work is to analyze the infrared images to determine the boundary layer transition location by the contrast on the wing, providing data for analyzing the impact of a pusher propeller on the laminar wing boundary layer. The effect of the pusher propeller at different angles of attack was analyzed and discussed. Based on the proposed setup capabilities and the experiment objectives, the experiments parameters were chosen as described in Table 2.

Table 2 – Experiment parameters

Angle of attack	$0^\circ < \alpha < 8^\circ$
Reynolds number	$Re = 4.5 \times 10^5$
Propeller advance ratio	$J = 0.3$

A low advance ratio ($J = 0.3$) was chosen for the experiments due to the higher impact on transition location at this condition, as indicated in the literature.
The transition line position detection uses the temperature gradient across the image in the chordwise direction, based on the image color intensity. The images were analyzed using Python code, which calculates the minimum derivative point. An example is shown in Figures 4 and 5. A Savitzky–Golay filter included on the SciPy library was used for reducing image noise and smooth the derivatives calculations. The results comparison shows that the filter application on the temperature distribution signal enables proper detection of the derivative minimum.

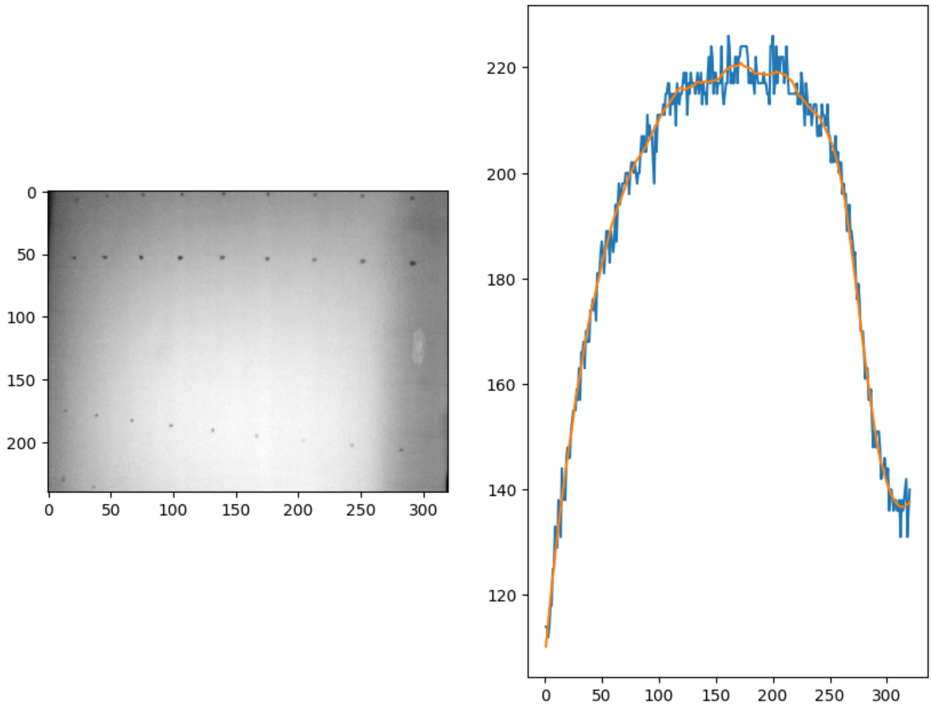

Figure 4 – Examples of raw image (left) and color intensity according to temperature distribution (right). The blue and orange lines represents the original and filtered signals respectively

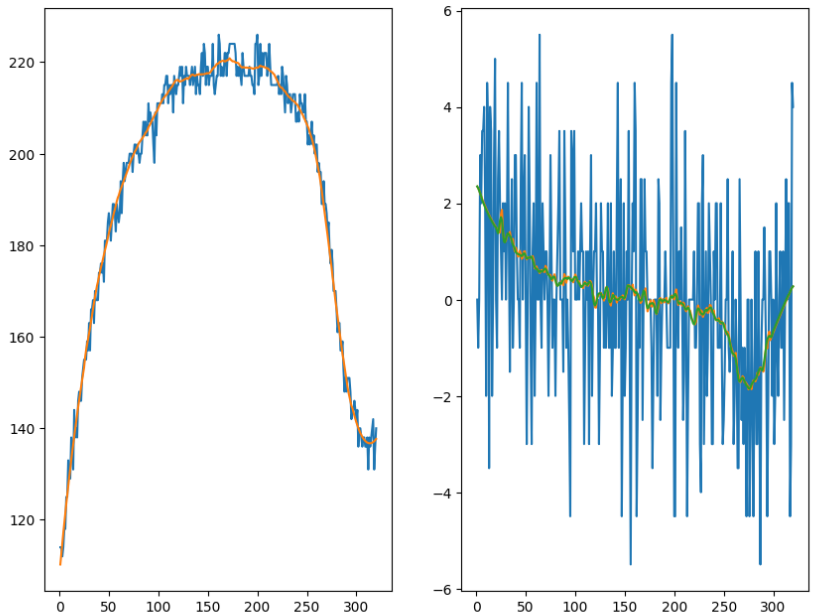

Figure 5 – Color intensity according to temperature distribution (left) and chordwise temperature derivative (right). The blue and orange lines are the derivative of the original and filtered signal derivatives and the green line is the filtered derivative

The transition points chordwise position was calculated using a bi-dimensional linear interpolation using the known position markers on the wing surface. The makers were drawn on the wing surface using a metallic ink pen, which reflects the infrared waves. The markers are seen as black dots on the images. The makers position is found using the Shi-Tomasi corner detection method implemented on the OpenCV Python library (Figure 6).

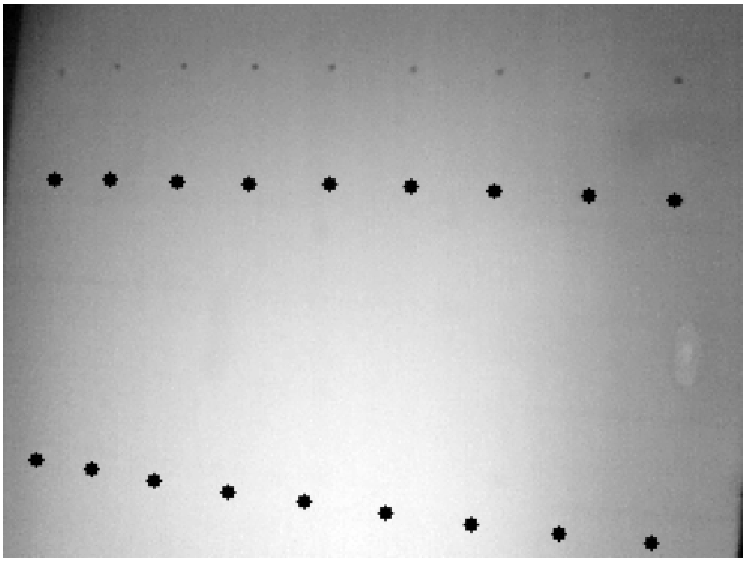

Figure 6 – Markers detected in the infrared image

The infrared images were analyzed using a Python code to detect the markers position and to determine and draw the transition line position (Figure 7).

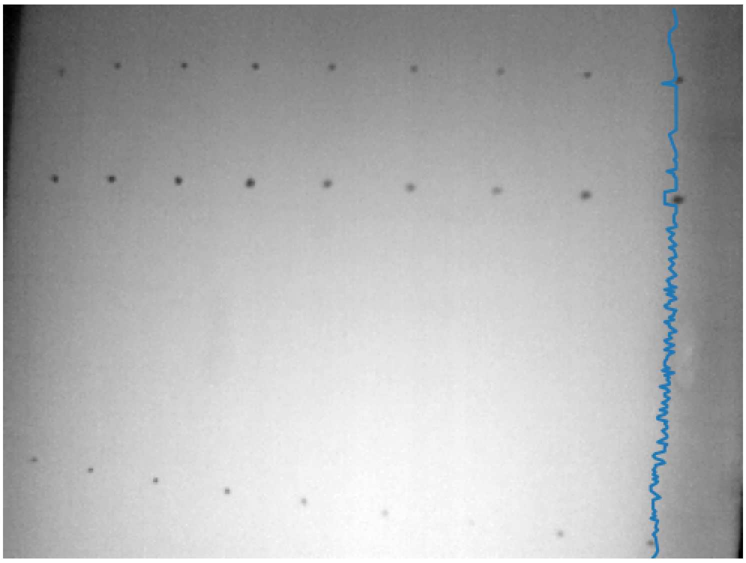

Figure 7 – Detected transition line

3. Results

The transition position was compared for the uninstalled propeller and the pusher propeller. The images of the transition location for $\alpha = 1°, 4°$ and $8°$ are shown on Figures to 8 to 10.

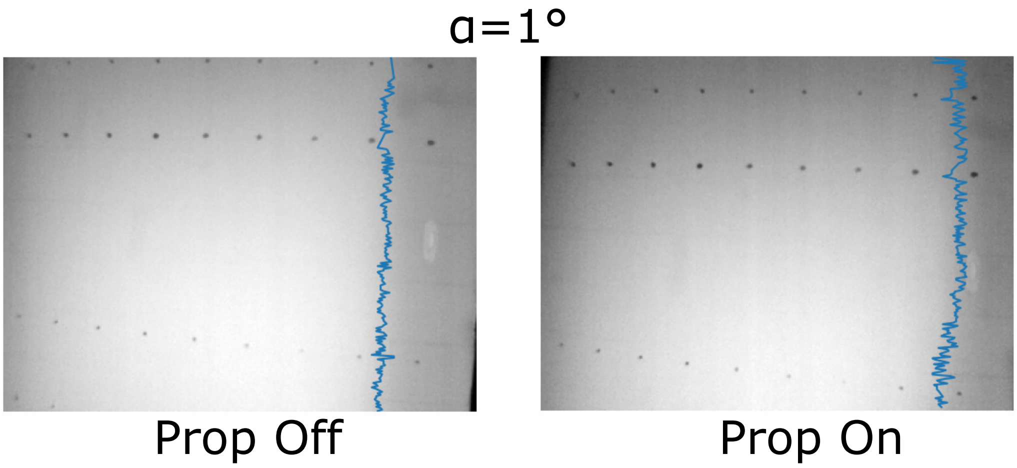

Figure 8 – Pusher propeller effect on transition line at $\alpha = 1°$ detected on the IRT experiments

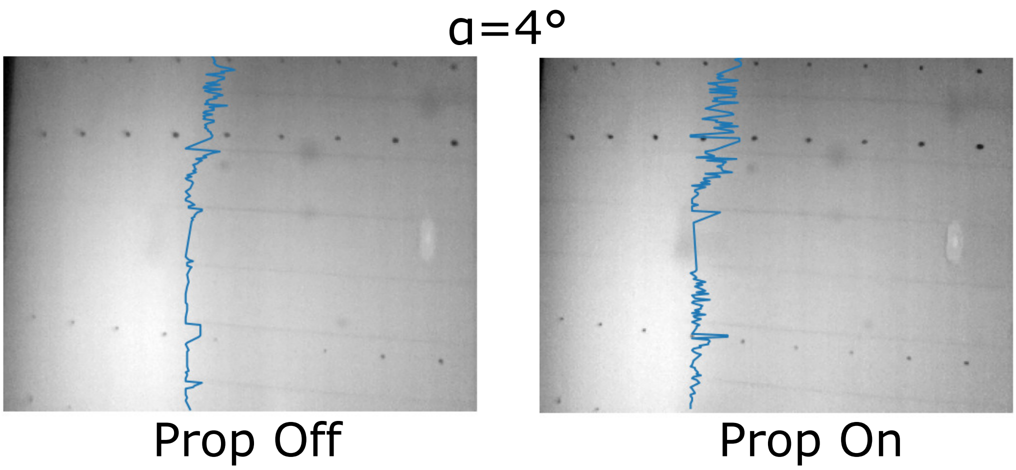

Figure 9 – Pusher propeller effect on transition line at $\alpha = 4°$ detected on the IRT experiments

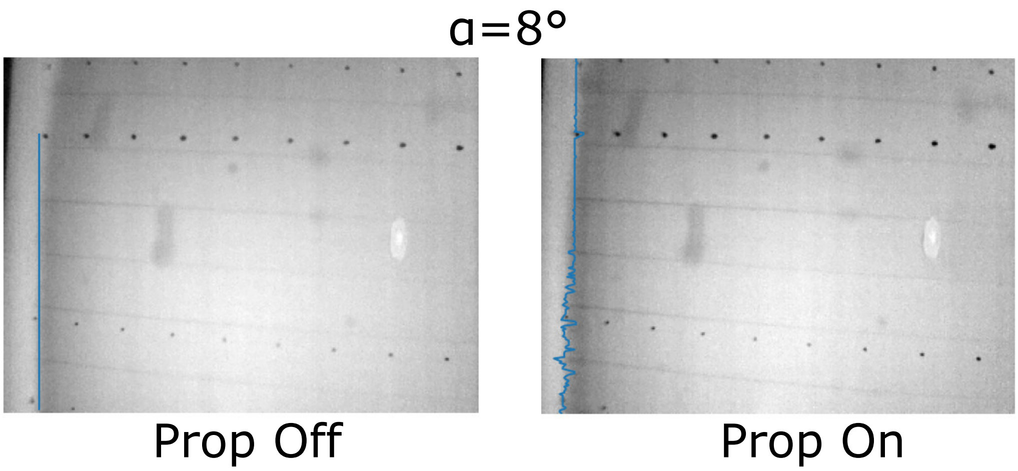

Figure 10 – Pusher propeller effect on transition line at $\alpha = 8°$ detected on the IRT experiments

The images indicate that the pusher propeller effect on the transition line is initially beneficial at $\alpha = 1°$. The propeller influence is reduced with the increasing angle of attack, reducing the laminar

boundary layer extension at $\alpha = 4°$ and is negligible at $\alpha = 8°$. This trend was already observed on previous works [13, 14, 15, 16]. It may be inferred that the further the transition line from the propeller actuation disk, the smaller its impact on the boundary layer transition position. Also, the images show that the proposed methodology detects and identifies the boundary layer transition front location.
To further understand the pusher propeller impact on the wing boundary layer transition location, the infrared images were analyzed to define the transition location at an angle of attack ranging from $\alpha = 0$ to $\alpha = 8$ as shown in Figure 11. The results confirmed that the pusher propeller has a beneficial effect at low angles of attack ($\alpha < 2$), increasing the laminar boundary layer extension, while an opposite effect occurs at higher values ($3 < \alpha < 5$). As the transition front closes to the leading edge ($5 < \alpha$), the propeller impact is reduced, resulting in a similar transition location for both configurations, being in accordance with previous results in the literature that studied a similar configuration using different techniques [13, 14, 15, 16]. These results indicate that a pusher propeller might provide better performance than tractor propellers by having a beneficial impact on a laminar wing boundary layer, enabling the usage of a natural laminar flow wing coupled with propeller-driven propulsion.

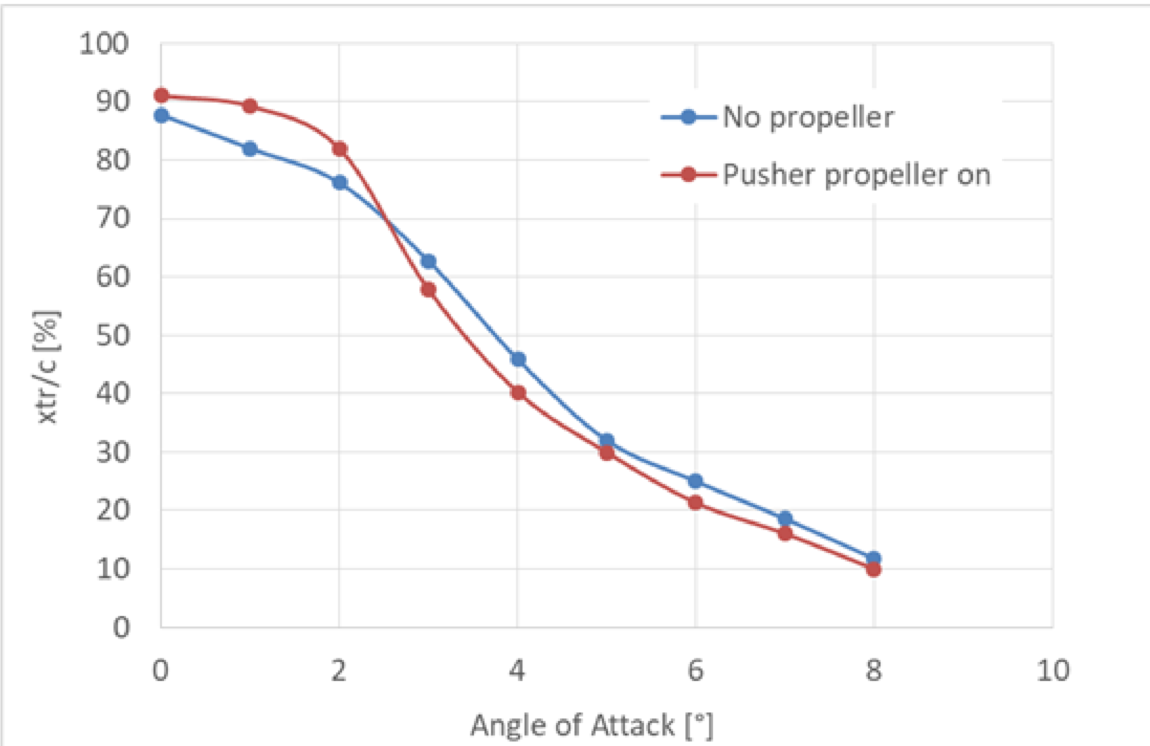

Figure 11 – Chordwise transition position for no propeller and propeller on configuration as function of angle of attack

4. Final remarks

This work presented an investigation on the impact of a pusher propeller on the laminar wing boundary layer using the infrared thermography technique. The proposed setup enabled measuring the boundary layer transition location without inserting instruments on the flow, reducing the instrumentation influence on the results.
The pusher propeller increased the laminar boundary layer extension at low angles of attack, with small or no reduction in its extension at higher angles. Also, there is an indication that the propeller impact on the laminar boundary layer extension is reduced as the transition front distances from the propeller action disk. In an analysis of the impact on aircraft performance, the results indicate that a pusher configuration might be a better option for a propeller-driven aircraft with wings designed for natural laminar flow compared to the tractor configuration.
Further investigation on the impact of the pusher propeller on wing aerodynamic coefficients correlated with the propeller position and advance ratio would contribute on evaluating the impact interac-

tion of the natural laminar wing and pusher propeller on a propeller-driven aircraft. Also, as indicated on the literature, the pusher propeller delays flow separation, increasing performance at high angles of attack. Future work on those topics are included on this work the research schedule.

5. Contact Author Email Address

mailto: joaopeguea@gmail.com

6. Acknowledgments

The authors thank the National Council for Scientific and Technological Development (CNPq) [grant number 147640/2019-9] for the financial support given to this research.

7. Copyright Statement

References

[1] International Civil Aviation Organization. *Resolution A40-18: Consolidated statement of continuing ICAO policies and practices related to environmental protection - climate change*, 2019. Available at: https://www.icao.int/environmental-protection/Documents/Assembly/Resolution_A40-18_Climate_Change.pdf. Access at: 09 feb. 2022

[2] International Air Transport Association. *Technology Roadmap*, 2013

[3] Schrauf G. Status and perspectives of laminar flow. *The Aeronautical Journal*, Cambridge University Press (CUP), v. 109, n. 1102, p. 639–644, dec 2005

[4] Holmes B J, Obara C J. Observations and implications of natural laminar flow on practical airplane surfaces. *ICAS Proceedings*. Seattle, 1982. v.1, p. 168–181. Available at: http://www.icas.org/ICAS_ARCHIVE/ICAS1982/ICAS-82-5.1.1.pdf. Access at: 09 feb 2022.

[5] Holmes B J, Obara C J. Observations and implications of natural laminar flow on practical airplane surfaces. *Journal of Aircraft*, American Institute of Aeronautics and Astronautics (AIAA), v. 20, n. 12, p. 993–1006, dec 1983.

[6] Holmes B J et al. Flight investigation of natural laminar flow on the bellanca skyrocket II. *SAE Technical Paper Series*, 1983.

[7] Holmes B J, Obara C J, Yip L P. *Natural laminar flow experiments on modern airplane surfaces*, 1984. Available at: https://ntrs.nasa.gov/api/citations/19840018592/downloads/19840018592.pdf. Access at: 09 feb. 2022

[8] Witkowski D, Johnston R, Sullivan J. Propeller/wing interaction. *27th Aerospace Sciences Meeting*, American Institute of Aeronautics and Astronautics, 1989.

[9] Witkowski D P, Lee A K H, Sullivan J P. Aerodynamic interaction between propellers and wings. *Journal of Aircraft*, American Institute of Aeronautics and Astronautics (AIAA), v. 26, n. 9, p. 829–836, sep 1989.

[10] Johnston R, Witkowski D P, Sullivan J P. Experimental results of a propeller/wing interaction study. *SAE Technical Paper Series*, SAE International, 1991.

[11] Ananda G K, Deters R W, Selig M S. Propeller induced flow effects on wings at low reynolds numbers. *31st AIAA Applied Aerodynamics Conference*, American Institute of Aeronautics and Astronautics, 2013.

[12] Ananda G K, Selig M S, Deters R W. Experiments of propeller-induced flow effects on a low-reynolds-number wing. *AIAA Journal*, American Institute of Aeronautics and Astronautics (AIAA), v. 56, n. 8, p. 3279–3294, aug 2018.

[13] Catalano F, Stollery J. The effect of a high thrust pusher propeller on the flow over a straight wing. *11th Applied Aerodynamics Conference*, American Institute of Aeronautics and Astronautics, 1993.

[14] Catalano F M, Stollery J L. The effect of a high thrust pusher propeller on the aerodynamic characteristics of a wing at low reynolds number. *International Congress of the Aeronautical Sciences - ICAS*, 1994. Available at: https://www.icas.org/ICAS_ARCHIVE/ICAS1994/ICAS-94-6.1.3.pdf. Access at: 10 feb. 2022

[15] Catalano F, Maunsell M. Numerical and experimental analysis of the effect of a pusher propeller on a wing and body. *35th Aerospace Sciences Meeting and Exhibit*, American Institute of Aeronautics and Astronautics, 1997.

[16] Catalano F M. On the effects of an installed propeller slipstream on wing aerodynamic characteristics. *Acta Polytechnica*, Czech Technical University Publishing House, 2004. Available at: https://ojs.cvut.cz/ojs/index.php/ap/article/view/562/394. Access at: 09 feb. 2022.

[17] Catalano F M. The new closed circuit wind tunnel of the aircraft laboratory of University of São Paulo, Brazil. *International Congress of the Aeronautical Sciences - ICAS*, 2004. Available at: http://www.icas.org/ICAS_ARCHIVE/ICAS2004/PAPERS/104.PDF. Access at: 09 feb. 2022.

[18] FLIR. *FLIR A300 Datasheet*, 2010. Available at: https://www.termokamery-flir.cz/wp-content/uploads/2013/09/Datasheet-Flir-A300.pdf. Access at: 10 feb. 2022.

[19] Joseph L A, Borgoltz A, Devenport W. Infrared thermography for detection of laminar–turbulent transition in low-speed wind tunnel testing. *Experiments in Fluids*, Springer Science and Business Media LLC, v. 57, n. 5, apr 2016.